ELSEVIER

Biochimica et Biophysica Acta 1321 (1997) 31–46

BIOCHIMICA ET BIOPHYSICA ACTA
BBA

Characterization of the *Rhodocyclus tenuis* photosynthetic reaction center

Ileana Agalidis [a,*], Anabella Ivancich [b,1], Tony A. Mattioli [b], Françoise Reiss-Husson [a]

[a] *Centre de Génétique Moléculaire, Bât. 24, CNRS, 91198 Gif-sur-Yvette Cedex, France*
[b] *Section de Biophysique des Protéines et des Membranes, Département de Biologie Cellulaire et Moléculaire, CEA and URA CNRS 2096, CEA / Saclay, 91191 Gif-sur-Yvette Cedex, France*

Received 6 February 1997; revised 24 April 1997; accepted 29 April 1997

Abstract

The photosynthetic reaction center (RC) from the purple non sulfur bacterium *Rhodocyclus tenuis* was isolated from membrane fragments by dodecyl dimethylamine oxide (LDAO) and purified by DEAE-chromatography in presence of dodecyl-maltoside (DM). The redox midpoint potential of the primary electron donor P was determined to be $E_m = 515$ mV $\pm$ 20 mV. The P^+ absorption band peaks at 1260 nm. Fourier transform resonance Raman spectra are consistent with a dimeric $(Bchl)_2$ structure of P where both acetyl carbonyl groups of P are hydrogen bonded, one with histidine, the other with a tyrosine residue. The primary quinone (Q_A) was identified to be menaquinone 8 and the secondary one (Q_B) ubiquinone 8. The secondary activity depends on the nature of the detergent. At pH 8 in DM solution, the rate of the $P^+Q_B^-$ back reaction is 0.1 s^{-1} and Q_B does not function as a two-electron gate. With LDAO addition, the rate became 0.3 s^{-1} and multiple binary oscillations of Q_B^- were observed. 10 μM orthophenanthroline blocks 50% of the electron transfer to Q_B ($I_{50} = 10$ μM). This high sensitivity was correlated with the nature of the residue at the position L226. © 1997 Elsevier Science B.V.

Keywords: Bacterial reaction center; Primary donor; Quinone; Resonance Raman spectra; (*Rhodocyclus tenuis*)

1. Introduction

Rhodocyclus (*Rc.*) *tenuis* is a facultative purple non sulfur bacterium which belongs, together with *Rc. purpureus* and *Rubrivivax* (*Rv.*) *gelatinosus*, to a separate group which is different from the other purple non sulfur bacteria. More precisely, it is classified in the β subclass of the Proteobacteria, according to the phylogenetic analysis based on the 16S ribosomal RNA [1,2]. One of the distinctive properties of *Rc. tenuis* concerns the morphology of its cell membrane, which is devoid of any invaginations; when cells adapt to photosynthetic growth conditions

Abbreviations: Bchl, bacteriochlorophyll; Bphe, bacteriopheophytin; Cyt, cytochrome; DAD, diaminodurene; DM, dodecyl maltoside; FT, Fourier transform; LDAO, lauryldimethylamine oxide; OD, optical density; P, primary donor; RC, reaction center; *C.*, *Chromatium*; *Cf.*, *Chloroflexus*; *Rsp.*, *Rhodospirillum*; *Rb.*, *Rhodobacter*; *Rc.*, *Rhodocyclus*; *Rv.*, *Rubrivivax*; *Rps.*, *Rhodopseudomonas*

* Corresponding author. Fax: +33 01 69823802; E-mail: agalidis@cgm.cnrs-gif.fr

[1] Present address: Spectroscopie des Complexes Polymétalliques et des Métalloprotéines, SCIB/DRFMC, CEA/Grenoble, 17 rue des Martyrs, 38054 Grenoble Cedex, France.

PII S0005-2728(97)00045-5

(which requires the insertion of the photosynthetic apparatus in the cytoplasmic membrane) they simply increase their size, and they do not develop chromatophores as in other purple bacteria [3]. In comparison with a large body of knowledge accumulated about the photosynthetic apparatus of purple non sulfur bacteria, few data are available for *Rc. tenuis*, but they indicate substantial differences. Original features of the light harvesting complexes (LHI and LHII) of *Rc. tenuis* have been described recently [4]; according to the sequences of its polypeptides, the peripheral antenna, LHII, appeared to be of a mixed character, being related both to LHI and LHII complexes of other purple bacteria. Like *Rps. viridis*, this bacterium contains a RC associated tetraheme Cyt *c* but having different values of its midpoint redox potentials ($E_{m1} = 385$ mV, $E_{m2} = 320$ mV, $E_{m3} = 115$ mV, $E_{m4} = 70$ mV) [5] and probably different heme orientations. On the other hand the presence of a variety of soluble electron transport proteins but the Cyt c_2 have been signaled in this bacterium, among which the high potential iron protein (HiPIP) [6], the three-dimensional structure of which is known [7]; recently, the direct involvement of HiPIP in the electron transport between the cytochrome bc_1 complex and the RC-associated tetraheme cytochrome has been demonstrated in *Rv. gelatinosus* [8] and also in *Rc. tenuis* (Verméglio, personal communication).

Currently, there is a great research interest in the membrane-diffusible quinones and soluble redox proteins mediating electron transport between cyt bc_1 and the reaction center (for a review, see Meyer and Donohue [9]). This has been recently stimulated with the finding that HiPIPs are directly involved in electron donation to RCs in such organisms as *Rv. gelatinosus* [8], *Rhodoferax fermentans* [10], *Rc. tenuis* (Verméglio, A., personal communication), as well as in *Chromatium inosum* [11]. Since HiPIPs are less efficient as electron donors than are those related to Cyt c_2 (common in Rhodospirillaceae), photosynthetic electron transport utilizing HiPIPs may be considered more primitive than those using Cyt c_2 (see Meyer et al. [12]). It is clear that to understand these electron transport processes, the redox proteins involved should be fully characterized. Towards this end, we have undertaken a comparative characterization of the *Rc. tenuis* reaction centers placing attention on the quinones and the primary electron donor, whose oxidation midpoint potential should be redox-compatible with the other proteins involved, such as the HiPIP and the RC-associated tetraheme.

Despite the phylogenetic distance between purple bacteria of the β and α-subgroups (the later including *Rhodobacter sphaeroides*, *Rb. capsulatus*, *Rhodospirillum rubrum*), a high homology exists at the level of their photosynthetic RCs, as seen by the sequence comparisons of the so-called L and M polypeptides of several purple bacteria, including *Rc. tenuis* [13]. It was thus assumed that a horizontal gene transfer occurred from an ancestor species of the α-subclass [14]. It is not known, however, if this homology extends to the third RC polypeptide, the so-called H subunit, which has not yet been sequenced for any species in the *Rhodocyclus* genera, and which is less strictly conserved than L and M in bacteria of the α-group.

In an effort to obtain a more detailed knowledge on the structure of RCs from the β-subclass of purple bacteria, several properties of the RC from R*v. gelatinosus* have been recently characterized [15], and differences have been observed in the energetics of the quinone acceptor complex, at the level of Q_A and Q_B, as compared to *Rb. sphaeroides* and *Rb. capsulatus*. In this work we extend our studies to *Rc. tenuis* and report the isolation and characterization of the RC from this bacterium. We have shown that its structural as well as functional properties share common features with bacterial RCs belonging to different branches of their evolutionary tree.

2. Materials and methods

2.1. Reaction center isolation

Rc. tenuis (strain ATTC 25093) was grown anaerobically in the light. The membrane fraction was isolated as described in [16] and was suspended at a concentration yielding an optical density in a 1-cm cuvette of 50 at 860 nm ($OD_{860} = 50$) in 0.1 M Na phosphate buffer pH 7.5 containing 9% glycerol and 5 mM Na ascorbate. This suspension was incubated in 3–4 mg/ml dodecyldimethylamine oxide (LDAO) (Fluka, Biochemica) for 1 h at 26°C. After centrifugation at $430\,000 \times g$ for 90 min the supernatant was

recovered; it contained crude RC and residual light harvesting antenna. Eventually, the pellets were resuspended and incubated again as above except that glycerol was omitted and the LDAO concentration was lowered to 0.9–1 mg/ml. Centrifugation was carried out at $200\,000 \times g$ for 90 min and a second supernatant containing RC was recovered. Both supernatants were combined and precipitated by ammonium sulfate (40% saturation) at 4°C for 20 min. The precipitate was recovered after 15 min centrifugation at $2000 \times g$ and suspended in a few mls of 0.1 M Tris-HCl pH 8 buffer, containing 0.1 M NaCl, 9% glycerol, 5 mM Na ascorbate and 0.4 mg/ml dodecyl maltoside (DM, Sigma). The solution was kept overnight at 4°C, and then desalted onto a PD10 (G-25 Sephadex, Pharmacia) column equilibrated with 10 mM Tris-HCl pH 8, 0.2 mg/ml DM. The sample was then adsorbed on a DEAE Sepharose column equilibrated with the same buffer, and eluted with a 0–0.27 M NaCl gradient. The RC was eluted at about 100 mM NaCl; fractions with absorbance ratios $A_{280\ nm}/A_{800\ nm}$ between 1.2 and 1.4 were pooled and concentrated by ultrafiltration (first on a Amicon XM50 membrane then with a Centricon 100 concentrating system).

2.2. Preparation of Q_B-depleted RC

A RC solution ($OD_{800} = 2$) was incubated in 10 mM Tris-HCl buffer, pH 8, in the presence of 8 mg/ml LDAO for 30 min at 30°C and then adsorbed on a DEAE-Sepharose column equilibrated with 10 mM Tris-HCl, 1 mg/ml LDAO, pH 8. In order to eliminate solubilized Q_B and degraded pigments, the column was successively washed with 3 vols. of equilibration buffer followed by 4 volumes of the same buffer but containing 0.2 mg/ml DM. Finally, the RC fraction was eluted with 0.3 M NaCl.

2.3. Extraction and identification of quinones

Quinones were extracted from *Rc. tenuis* membrane fragments and lipids were removed using a modified Bligh and Dyer method as described in [17]. Extracts were chromatographed on activated (30 min, 120°C) HPTLC silica gel plates (Merck) developped with petroleum ether/diethyl-ether 85/15 (v/v). Spots were revealed by UV fluorescence and I_2 staining, and identified as ubi- or menaquinones by comparison with UQ_8 and MK_8 (Hofmann La Roche) chromatographed in parallel.

We observed that quinone analysis in reaction center samples required removal of DM before extraction. Thus the samples were freed from detergent by overnight treatment at 5°C with Biobeads SM-2 (Biorad); the beads were eliminated by filtration and the turbid reaction center samples were analyzed as above.

2.4. FPLC gel filtration

The apparent molecular weight of the detergent-RC complex was determined on a Superose 12 HR 10/30 column (Pharmacia), equilibrated with a 50 mM Tris-SO_4H_2 buffer containing 50 mM SO_4Na_2 and 0.2 mg/ml DM. A 100 μl RC sample was injected and eluted with the same buffer at 0.5 ml/min. Absorbance at 410 nm was followed with a Beckman 160 absorbance monitor. In some runs, 100 μl fractions were collected and their absorption spectra were recorded with a Cary 2300 spectrophotometer. Calibration of the column was done with water-soluble proteins (thyroglobulin, catalase, transferrin, ovalbumin, and myoglobin).

2.5. Electrophoresis

SDS-polyacrylamide gel electrophoresis was carried out [18] on minigels with 12.5% polyacrylamide in the resolving gel and 4% in the stacking gel. Heme staining was performed [19], then the gel was destained and stained further with Coomassie Blue R250 or silver.

2.6. Spectral measurements

Absolute and differential absorption spectra were recorded on a Cary 2300 spectrophotometer equipped for cross-illumination; concentration of the RC was determined from the absorbance in the Q_y band using the extinction coefficient measured for *Rb. sphaeroides* RC [20]. Tetrahemic Cyt *c* content was estimated by assuming a value of 96 $M^{-1} \cdot cm^{-1}$ for the global differential absorption coefficient in the Cyt α-band ($\Delta\epsilon_{red\text{-}ox}$ (553 nm − 538 nm), corresponding to four hemes per cytochrome [21]. Redox

titrations of membrane fragments were carried out by using a flow cell with an external reaction vessel. The light-induced absorbance changes due to the donor P/P^+ were measured between 850 and 900 nm at a series of ambient redox potentials, monitored by a combined Ag/AgCl-Pt electrode (Ingold). The electrode was calibrated using saturated quinhydrone solutions prepared at pH 5 and 7.4 as described elsewhere [22]. Low-temperature (77 K) absorption spectra were recorded on a Aminco-Chance DW2 spectrophotometer. Flash experiments were done on a home-made single beam spectrophotometer [23].

Near-infrared Fourier transform (FT) resonance Raman spectra of isolated RCs were recorded using a Bruker IFS 66 interferometer coupled to a Bruker FRA 106 Raman module equipped with a continuous, diode-pumped Nd:YAG laser [24]. Reaction center samples were measured at both room and low temperature (10 K) and were excited with 180 mW and 200 mW of 1064 nm laser radiation, respectively. For the low temperature experiments, the samples were held in a gas flow cryostat (SMC-TBT, France) regulated by the circulation of cold helium gas. The spectral resolution was 4 cm^{-1}. The minor fluorescent backgrounds of the spectra were corrected by a polynomial fit and the maxima of the Raman bands were determined both by deconvolution and second derivative analyses.

For the FT Raman experiments, RC samples were concentrated to ca. 100 OD at 867 nm using a Centricon microconcentrating system (Amicon) and were poised to their reduced (P) or oxidized (P^+) states with sodium ascorbate or potassium ferricyanide, respectively.

3. Results

3.1. Isolation and composition of Rc. tenuis RC

Rc. tenuis RC was solubilized from cytoplasmic membrane fragments with LDAO, precipitated by ammonium sulfate and purified in presence of DM by anion exchange chromatography. A typical optical absorption spectrum of purified RCs is shown in Fig. 1 and displays characteristic near-infrared absorption bands at 868, 801, and 753 nm corresponding to the Q_y transitions of the primary donor (see below), the

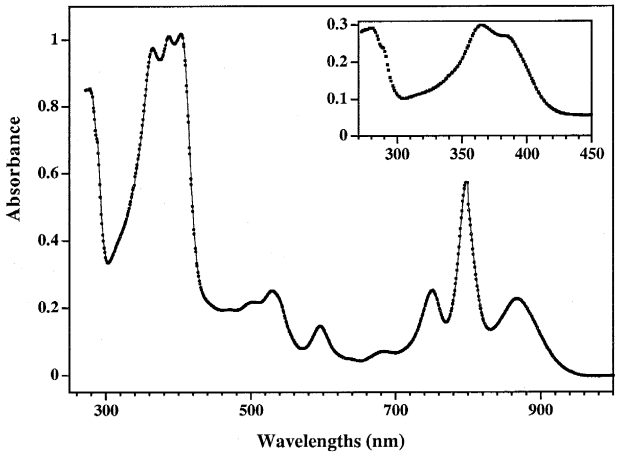

Fig. 1. Optical absorption spectrum of *Rc. tenuis* RCs in 10 mM Tris, pH 8, 0.2 mg/ml DM; in this sample 0.4 tetraheme Cyt *c* was still associated per RC. Inset: another sample where only 0.1 Cyt *c* was bound per RC.

accessory Bchls, and Bphes, respectively as well as a band at 597 nm corresponding to the Q_x transition of Bchls. Other bands are observed at 532 nm (carotenoid and Bphe), 496 nm (carotenoid) and at 404, 386 and 366 nm. These latter three bands are attributed to the Soret transitions of the hemes, Bphes, and Bchls respectively. The above spectral features are very similar to those of other purified RCs which contain *a*-type bacteriochlorins and carotenoid, such as *Rb. sphaeroides* [25]. The strong similarity of the optical absorption spectrum and of the relative intensities of the Q_y absorption bands of P, Bchls and Bphes with those of *Rb. sphaeroides* RC, strongly suggest that the Bchl *a*/Bphe *a* ratio in the *Rc. tenuis* RC is 2:1 and that the general arrangement of these pigments is similar for these two RCs. Identification of the carotenoid molecule(s) bound to the RC is currently under study.

Besides the two peaks (366 and 386 nm) belonging to Bchls and Bphes, the Soret spectral region shows an extra peak at about 410 nm likely due to a tetraheme cytochrome *c* associated to the RC. The presence of a tetraheme Cyt *c* has already been reported in this bacterium [5]; association of such a cyt with the RC has been observed in other purple bacteria [26]. A gradual loss of Cyt *c* during the isolation procedure was observed and was likely due to the detergent treatments (by LDAO and DM) as well as to ammonium sulfate precipitation. In purified

RC preparations the content of Cyt *c* per RC was variable in the range 0.1–0.4; in Fig. 1, 0.4 tetraheme cytochrome *c* was present per RC whereas in another preparation (shown in the inset of Fig. 1) only 0.1 Cyt *c*/RC was left. During further analysis of a RC sample by HPLC gel filtration, the RC was eluted in a single peak but a variable cyt/RC ratio was observed across the elution peak itself; thus the unbinding of cyt was still occurring during chromatography. Despite this somewhat loose association, in a RC sample prereduced by DAD/ascorbate, the residual Cyt *c* was still photooxidized by the RC, as demonstrated by multiflash experiments (data not shown).

When *Rc. tenuis* RCs were isolated and purified in the presence of LDAO they were less stable than in DM, as observed by a fast, irreversible decrease of the donor Q_y absorption band and by the pheophytinisation of the Bchl (data not shown). Therefore LDAO was used only for extracting the RC from the membrane fragments, and DM was used for purification on column. However, even in the presence of DM the RC underwent a partial degradation after 2–3 weeks at 4°C, detected by a decrease in amplitude of the donor Q_y absorption band (data not shown).

By HPLC gel filtration in presence of DM the apparent M.W. of the native RC-detergent complex was estimated to be 150 kDa. After SDS denaturation, the electrophoretic pattern of purified RC indicated the presence of three polypeptides with apparent M.W. of 25, 29 and 36 kDa which likely corresponded to L, M, and H subunits respectively (Fig. 2). Another weak component of 43 kDa was not stained by Coomassie blue and revealed only by heme staining and by silver staining. It was attributed to the residual tetraheme Cyt *c* polypeptide.

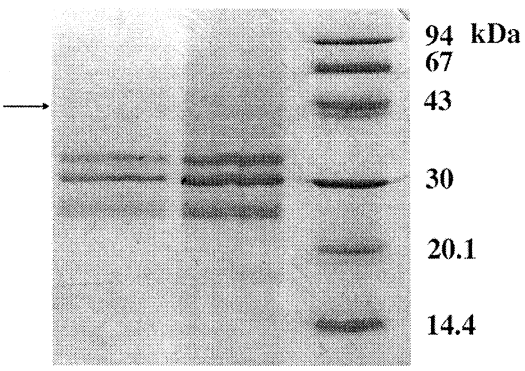

Fig. 2. SDS gel electrophoresis of purified *Rc. tenuis* RC (two left lanes, differing by loads) and marker proteins (right lane). The gel was stained with Coomassie blue; the arrow shows the position of the cytc polypeptide, previously revealed by heme staining.

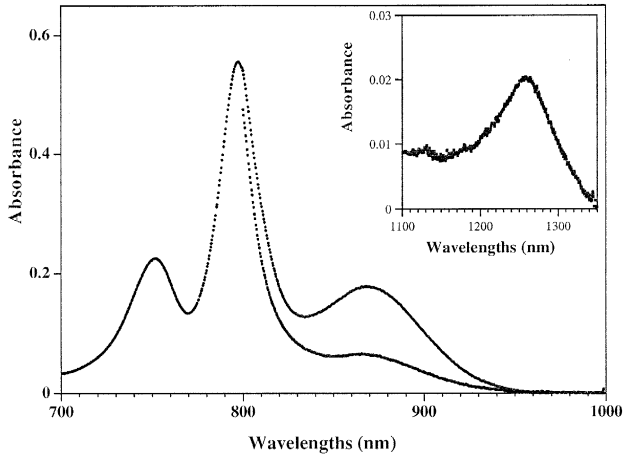

Fig. 3. Near-IR absorption spectra of purified RC recorded in the dark and continuous light, respectively. The photooxidation of the donor is indicated by a simultaneous bleaching at 870 nm and the rise of a weak absorption band at 1260 nm. The unbleached fraction is due to Q_B-depleted RCs, as we observed by a total bleaching after UQ_6 and LDAO addition (not shown).

3.2. Spectral and redox properties of the primary donor

Photochemical activity was verified in the isolated RC by the light-induced bleaching of the primary donor band at 867 nm and the simultaneous appearance of an absorption band at 1260 nm, attributed to the cation radical P^+ (see Fig. 3). This latter band was shifted 10 nm to longer wavelength (see inset of Fig. 3) relative to the 1250 nm P^+ band determined in *Rb. sphaeroides* RC [27]. The ratio of the absorbance maxima at 868 nm (in state P) and 1260 nm (in state P^+) was about 10, similar to what has been observed for *Rb. sphaeroides* and *Rsp. rubrum* RCs [28]. At 77 K the Q_y band maximum was observed at 894 nm (data not shown), which is slightly red-shifted with respect to its position in *Rb. sphaeroides* RC, i.e., 890 nm. In the room temperature light-minus-dark spectrum of *Rc. tenuis* membrane fragments, the maximum bleaching of the dimer Q_y band was located at 890 nm, which corresponded to a 23 nm red-shift relative to its position in isolated RC. This

Table 1
Comparison of several properties of *Rc. tenuis* RC with other known bacterial RCS

Bacterium (class)	$E_m(P^+/P)$ (mV) [a]	H-bond donor to P_L [b]	H-bond donor to P_M [c]	Q_A [d]	Q_b [e]	I_{50} μM [f]	Residue L226 [g]
Rc tenuis β	515 *	His * *	Tyr * *	MK_8	UQ_8 *	10 *	Ala * *
Rv. gelatinosus β	400 [76]	His 168 [32,81]	none	MK_8	UQ_8 [18]	3 [51]	Ser [81]
C. tepidium γ	502 [34]; (526) [34]	His L137 [34]	Tyr M196 [34]	MK_7	UQ_7 [47]	n.d.	n.d.
Rps. viridis α	500 [77]; (520) [78]	His L168 [57,66]	TyrM195 [57,66]	MK_9	UQ_9 [52]	30 [50]	Ala [57,66]
Rb. sphaeroides α	450 [31] *; (495) [67,29]	His L168 [6,63,65]	none	UQ_{10}	UQ_{10} [25]	200 [52]	Thr [63,24]
Cf. aurantiacus	420 [79]; (386) [80]	none Phe L207 [82]	Tyr M183 [82]	MK_{10}	MK_{10} [83]	n.d.	n.d.

n.d., not determined.
[a] P/P^+ redox midpoint potential of the primary donor (between pH 7 and 8) in membrane fragments (and in isolated RCs); (in b and c subscripts the amino acid residues were identified in *Rps. viridis* and *Rb. sphaeroides* crystallographic structures, and inferred from primary sequences and FT Raman data for the other bacteria).
[b] H-bond donor to the C_2 acetyl carbonyl group of the Bchl of P associated with the L subunit; [c] H-bond donor to the C_2 acetyl carbonyl group of the Bchl of P associated with the M subunit; [d] chemical nature of the Primary quinone; [e] chemical nature of the secondary quinone; [f] o-phen concentration required to inhibit the electron transfer between Q_A^- and Q_B at 50 percent; [g] amino acid residue at position L226 (*Rb. sphaeroides* numbering) which is related to the degree of inhibition by o-phen (see text).
* This work; * * Nagashima personal communication.

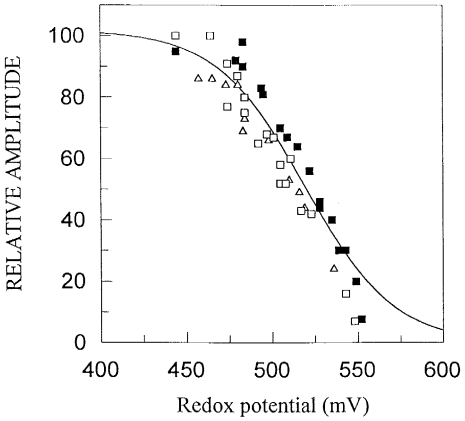

Fig. 4. Chemical redox titration of light-induced absorbance changes of P in *Rc. tenuis* cytoplasmic membranes suspended in 50 mM Tris-HCl buffer pH 8. Potassium ferricyanide and sodium dithionite were added in order to increase and decrease respectively the redox potential of the cytoplasmic membranes suspension prior to illumination. Closed rectangles: oxidative titration; open rectangles and triangles: reductive titration. The line represents the fit of the data to the Nernst equation ($n = 1$). The calculated midpoint potential is (515 ± 15) mV.

large difference could reflect specific interactions of the RC with its lipoproteic environment within the membrane, which drastically changed once the RC was extracted and solubilized by the detergent [29], and/or the RC-associated tetraheme cytochrome [30].

In order to determine the electrochemical properties of the donor, we measured the redox midpoint potential of P in *Rc. tenuis* cytoplasmic membranes by measuring light induced absorbance changes due to P^+ formation at different redox states (Fig. 4) as well as that in *Rb. sphaeroides* chromatophores for comparison. A redox titration could not be performed on isolated *Rc. tenuis* RC because P was gradually damaged during the oxidative treatment. In these measurements the tetraheme cytochrome remains fully oxidized and thus cannot interfere by reducing P^+. A value of $E_m = 515 \pm 20$ mV at pH 8 was obtained for the P/P^+couple in *Rc. tenuis* membranes (see Fig. 4), as compared to 450 mV in *Rb. sphaeroides* strain Y chromatophores (not shown), this latter value being in good agreement with that already published [31]. Thus the midpoint redox potential of the donor is about 70 mV higher in *Rc. tenuis* than in *Rb. sphaeroides* chromatophores (Table 1).

3.3. Near-infrared FT resonance Raman spectra of the reduced (P) and oxidized (P^+) Primary Donor of Rc. tenuis

As mentioned before, the electronic absorption spectrum of *Rc. tenuis* RC (Fig. 1) is similar to that of *Rb. sphaeroides*, with an absorption maximum at ca. 870 nm arising from P and a P^+ absorption band at 1260 nm. Thus, under our experimental conditions, we can expect a selective (pre)resonance Raman enhancement of the primary donor, P (via its 870 nm absorption transition) in the FT Raman spectrum of reduced *Rc. tenuis* RCs excited with 1064 nm, similar to that observed for the dimeric primary donors in RCs of *Rb. sphaeroides* ([24] and other Bchl a-containing RCs [30,32–34]. Bands in the FT Raman spectra of RCs poised in their neutral P state which bleach upon P^+ formation are attributable to P while those new bands appearing in the P^+ FT Raman spectra (due to a genuine resonance enhancement via the 1260 nm transition) are assignable to P^+ [24,30,32–36].

Fig. 5 shows the room temperature FT (pre)resonance Raman spectrum of *Rc. tenuis* RCs, in the 1550–1800 cm^{-1} spectral region, excited with 1064 nm light and in both the reduced P (Fig. 5A) and oxidized P^+ (Fig. 5B) states. In Fig. 5A the bands at

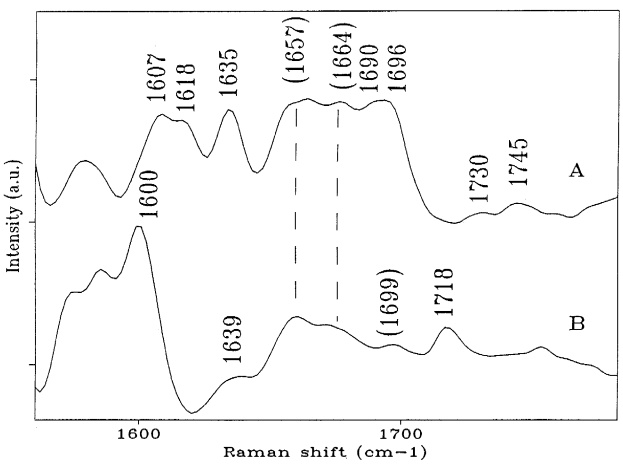

Fig. 5. Room temperature FT Raman spectra of *Rc. tenuis* RCs excited with 1064 nm laser radiation, and poised in their P (A) and P^+ (B) states. The 1550–1800 cm^{-1} spectral region shown includes the vibrational stretching modes of the C_aC_m methine bridges and the conjugated carbonyl groups of the primary donor.

1607, 1618, 1635, 1694 (broad), 1730, and 1742 cm^{-1}, all disappear upon P^+ formation, and thus can be assigned to P. Similarly, in Fig. 5B the bands at 1600, 1639, and 1718 cm^{-1}, clearly appear upon P^+ formation, and thus are assigned to P^+. Conversely, the bands at 1657 cm^{-1} and 1678 cm^{-1} that are present in the P spectrum and persist in that of P^+ should not then arise from P. They most probably arise from protein, the monomeric Bchl molecules, or Bphe molecules contributions, respectively [29,30,34,35]. The weak band at 1699 cm^{-1} in the P^+ spectrum (Fig. 5B) might have been masked underneath the broad 1694 cm^{-1} band in P spectrum, and thus cannot be unambiguously attributed to P.

In Fig. 5A, the 1607 cm^{-1} band is consistent with the vibrational frequency of the CaCm methine bridge stretching modes of pentacoordinated Bchl molecules [37]. A similar band was observed in the P FT Raman spectrum of *Rb. sphaeroides* RCs [24] and assigned to the CaCm methine bridge stretching modes of both Bchl molecules constituting P, each with a single histidine axial ligand. The axial ligands of the Bchl molecules of the *Rc. tenuis* primary donor are, presumably, also histidine residues.

The Raman vibrational frequencies of the π conjugated carbonyl groups of P are expected to be observed in the spectral region of ca. 1620 cm^{-1} (H-bonded) to 1660 cm^{-1} (free) if arising from C_2 acetyl carbonyls, and at ca. 1660 cm^{-1} (H-bonded) to 1700 cm^{-1} (free) if arising from C_9 keto carbonyl groups [38]; the magnitude of the shift in frequency of these carbonyl group vibrators is indicative of the strength of the H-bond interaction. The bands at 1618 cm^{-1} and 1635 cm^{-1} in the P spectrum of *Rc. tenuis* in Fig. 5A are only consistent with two C_2 acetyl carbonyl groups, both engaged in H-bonds of different strengths, and the broad band at 1694 cm^{-1} is consistent with a free C9 keto carbonyl group. The 1618 cm^{-1} band is reminiscent of the 1620 cm^{-1} band seen in the P FT Raman spectrum of *Rb. sphaeroides* RCs and which was assigned to the P_L C_2 acetyl carbonyl which is H-bonded to His L168 [24,35]. The second, H-bonded, C_2 acetyl group in *Rc. tenuis* is observed at 1635 cm^{-1}, which is 18 cm^{-1} lower in frequency than the 1653 cm^{-1} band in the P FT Raman spectrum of *Rb. sphaeroides* assigned to the non-H-bonded C_2 acetyl carbonyl of P_M [24,35]. This difference in vibrational frequency is due to the difference in H-bonding states of the homologous P_M acetyl groups of these two species. Comparable frequency shifts were observed when H-bonds were genetically introduced or broken on the C_2 acetyl carbonyl groups of the primary donor of *Rb. sphaeroides* [35,36,39]. The broad band at ca. 1694 cm^{-1} was found to be composed of 1690 and 1696 cm^{-1} components (by second derivative and deconvolution analyses), and resembles the 1696 and 1697 cm^{-1} bands in the P FT Raman spectra of *Cf. aurantiacus* [34] and *C. tepidum* RCs [30], respectively, which were also both composed of two nearly degenerate bands assigned to the two C_9 keto carbonyls of their respective primary donors. The situation is different for *Rb. sphaeroides* where the P_M and P_L free C_9 keto carbonyls vibrate at distinctly different frequencies, 1679 and 1691 cm^{-1}, respectively [24,35]. Finally, the weaker bands at 1730 cm^{-1} and 1745 cm^{-1} resemble those observed in the FT Raman spectrum of *Rb. sphaeroides* P, most likely arising from the C_{10} carbomethoxy ester carbonyl groups [24].

In summary, the FT Raman data reveal that the primary donor of *Rc. tenuis* is constituted of Bchl molecules which possess two free C_9 keto carbonyl groups and two H-bonded C_2 acetyl carbonyl groups. This H-bond pattern is different from that of *Rb. sphaeroides* where only the P_L C_2 acetyl carbonyl of P is engaged in a H-bond (Table 1). The fact that bands attributable to four conjugated carbonyl groups are observed in the P FT Raman spectrum of *Rc. tenuis* RCs indicates that the primary donor is constituted of more than one and most likely of two excitonically coupled Bchl molecules as it is in *Rb. sphaeroides* RC [24]. The single 1607 cm^{-1} band seen in Fig. 5A indicates that both Bchl molecules constituting the *Rc. tenuis* primary donor are coordinated by one axial ligand each, most likely histidine, as is the case for all known RCs to date.

3.4. Quinone acceptor complex

For *Rc. tenuis*, the presence of ubiquinone (UQ) and menaquinone (MK), both with a chain of eight isoprenoid units, has already been demonstrated [40]. Extraction and analysis of quinones from intact and from Q_B-less RCs allowed us to identify Q_A as MK_8 and Q_B as UQ_8.

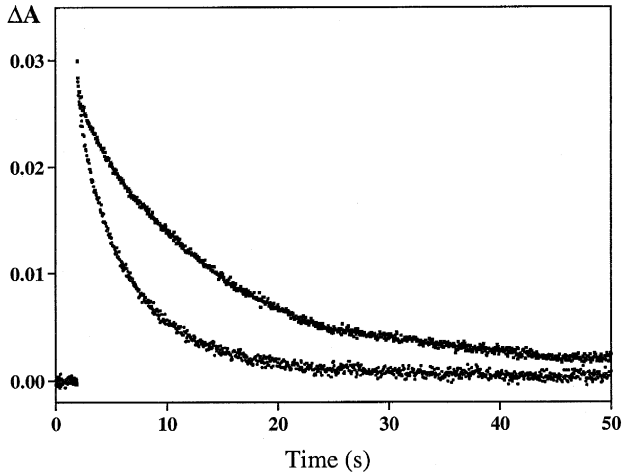

Fig. 6. Flash-induced absorption changes and decay at 430 nm of 2.7 μM RC solution in Tris buffer pH 8, containing 0.2 mg/ml DM ($\tau = 10$ s). Lower trace: after addition of 1 mg/ml LDAO ($\tau = 3.3$ s).

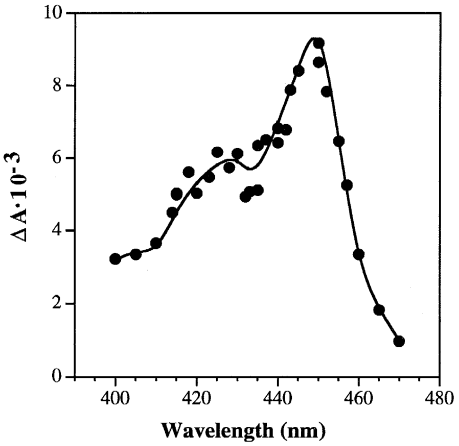

Fig. 7. Flash-induced difference spectrum of semi-ubiquinone Q_{B-} in presence of DM; same conditions as in Fig. 6 except that 1 mM DAD was added.

A single flash illumination of a solution of intact RCs containing 0.2 mg/ml DM elicited the formation of $P^+Q_B^-$ radical pair, which recombined with a mean time, τ, of about 10 s (Fig. 6, upper trace). In typical RCs preparations the Q_B site occupancy was 80–90%. In order to determine if the nature of the detergent modified the kinetics of P^+ rereduction, we tested RC solutions containing either Na cholate, Deriphat 160, $C_{12}E_8$, or LDAO (at pH 8). Among these detergents, only LDAO (0.5–1 mg/ml) induced a change in the back reaction time relative to DM, accelerating P^+ decay to about $\tau = 3$–4 s (see Fig. 6, lower trace). In membranes, P^+ rereduction is faster, occuring with a mean time of 1–2 s only (not shown), a value close to that found in *Rb. sphaeroides* RCs.

In a RC sample containing DM and diaminodurol (a rapid reductant of P^+ which prevents the $P^+Q_B^-$ back reaction to occur) a single flash excitation led to the formation of $PQ_AQ_B^-$ state with a rather long lifetime (20–30 min). Fig. 7 shows the flash-induced absorption profile of Q_B^- measured at least 1–2 s after the excitation flash; under these conditions there is no contribution of the residual tetraheme cytochrome to the Q_B^- absorption band, as the photooxidized high potential heme is rapidly rereduced by DAD (within 30–70 ms) after the flash. This absorption profile is typical of a semi-ubiquinone radical photoinduced in other bacterial RCs and playing the role of secondary electron acceptor [41,42] When an excess of UQ_6 was added, a train of saturating flashes induced a single oscillation of Q_B^- as if hydroquinol formed after the second flash could not exchange with the exogenous quinone pool (not shown). However, if LDAO (0.5–1 mg/ml) was added to such a sample, multiple Q_B^- binary oscillations were observed, similar to those shown in Fig. 8. These observations suggested that: (1) in the absence of LDAO, UQ_6 molecules were trapped inside the bulky dodecyl maltoside micelles, preventing them to exchange with ubiquinol formed at the Q_B site; (2) the

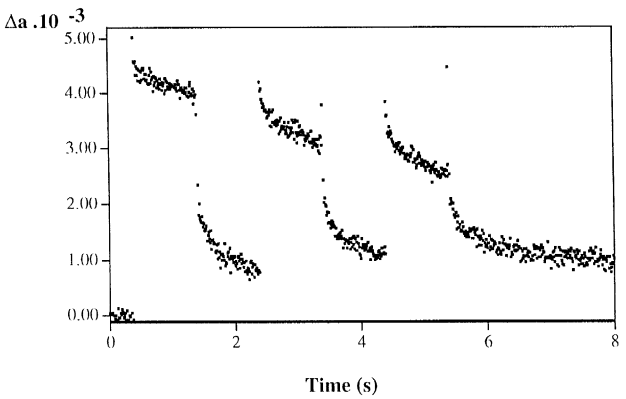

Fig. 8. Binary oscillations of semi-ubiquinone (Q_B^-) observed at 450 nm in RCs after a series of saturating flashes. RCs were suspended in 10 mM Tris buffer pH 8 containing 0.5 mg/ml DM, 1 mg/ml LDAO, 40 μM UQ_6 and 1 mM DAD.

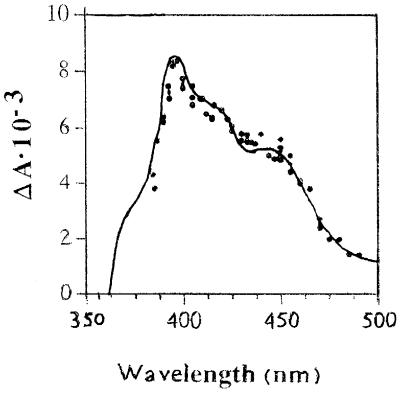

Fig. 9. Flash-induced difference spectrum (closed points) of semi-menaquinone Q_A^- obtained in presence of 500 mM DAD in Q_B-less RCs; same conditions as in Fig. 7. For comparison the flash-induced difference spectrum published for semimenaquinone Q_A^- in *Chl. aurantiacus* RC (continuous line) [43] has been superposed but with a 5 nm red shift as to get the same position of the maximum.

addition of LDAO led to the formation of smaller LDAO and/or DM/LDAO mixed micelles, facilitating the diffusion of UQ_6 into the protein and the regeneration of oxidized Q_B.

In *Rc. tenuis* RCs, incubation with LDAO (8 mg/ml as described in Section 2) resulted in an easy extraction of 85% of the secondary quinone. The absence of Q_B was checked by the back reaction rate which was the same as in the presence of herbicide ($k_a = 28\ s^{-1}$) (see below). A gradual recovery of secondary activity (up to 80%) took place after incubation of Q_B-depleted RCs with an excess of UQ_6, provided that LDAO (0.5–1 mg/ml) was added to the RC solution already containing DM. This was demonstrated by a decrease in the P^+ rereduction rate after a flash ($k_b = 3.3\ s^{-1}$) and the concomitant appearance of multiple flash-induced binary oscillations of Q_B^- observed at 450 nm in the presence of DAD (see Fig. 8). It is of note that secondary activity could not be reconstituted in a DM solution in the absence of LDAO; this fact confirms our hypothesis that quinones cannot be exchanged between DM micelles and the protein.

Identification of Q_A required the measurement of Q_A^- absorption spectrum without the eventual interference of the secondary quinone Q_B. Thus we used Q_B^- depleted RCs for these measurements. In these samples, the state PQ_A^- was formed with the same conditions as above, i.e., by flash excitation in the presence of diaminodurol. The flash-induced absorption spectrum (Fig. 9) has a striking resemblance with that reported for the semi-menaquinone identified as Q_A^- in *Cf. auriantacus* and in *C. vinosum* RCs [43,44]. Its maximum is located at 395 nm, thus close to the maximum of semi-menaquinone in vitro [45]. However it displays slightly different spectral features relative to the semi-menaquinones bound to *Rps. viridis* and *Rv. gelatinosus* RCs, where the maxima are red-shifted to 412 nm [18,46].

3.5. Herbicide sensitivity

Terbutryn and orthophenanthroline (o-phen), which are known to block the electron transfer between the two quinones, were tested on *Rc. tenuis* RC. In the presence of these herbicides, the flash induced $P^+Q_A^-$ radical pair relaxed with a mean time $\tau = 35$ ms (not shown). This fast recombination time is close to the values measured in isolated bacterial RCs which have menaquinone as Q_A and ubiquinone as Q_B [18,47,48].

The sensitivity to o-phen was measured in membrane fragments as well as in isolated RCs (see Fig. 10); the inhibitor concentration required to reduce Q_B activity to 50%, $I_{50} = 10\ \mu M$, is within the range of values determined for *Rps. viridis* [49,50] and *Rv. gelatinosus* RCs [51] (Table 1). The inhibition power of this herbicide was about 10 times smaller in *Rb. sphaeroides* and *Rb. capsulatus* RCs [52–54]. The sensitivity to terbutryn was determined in isolated *Rc. tenuis* RC; the value of I_{50}, 5 μM, is close to

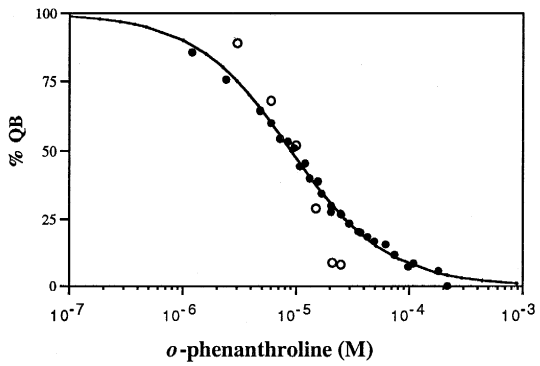

Fig. 10. Inhibition of electron transfer from Q_A^- to Q_B by o-phen in cytoplasmic membranes (closed points) and in isolated RCs (open points); $I_{50} = 10\ \mu M$.

Table 2
Detergent effects upon various kinetic parameters in isolated *Rc. tenuis* RCs: k_b, the $P^+Q_AQ_B^-$ recombination rate; K_2, the apparent equilibrium constant between Q_AQ_B and $Q_AQ_B^-$ states, and ΔG, the free energy difference between these states

Detergent	k_b (s^{-1})	K_2	$-\Delta G$ (mV)
$C_{12}M$ (0.2 mg/ml)	0.1	300	134
$C_{12}M$ (0.2 mg/ml) + $C_{12}DAO$ (0.5 mg/ml)	0.2	142	117
$C_{12}M$ (0.2 mg/ml) + $C_{12}DAO$ (1 mg/ml)	0.33	86	105
Membrane fragments	0.66–0.5	42–50	92

Values of these parameters measured in membrane fragments are shown for comparison.

those already determined for *Rps. viridis* [46,50] and *Rb. sphaeroides* [52].

3.6. Energetics of quinone acceptor complex in Rc. tenuis; dependence on detergents

The rate of $P^+Q_A^-$ recombination has the same value in isolated RC as in membrane fragments ($k_a = 28\ s^{-1}$) irrespective of the kind of detergent present in the RC solution (not shown). In contrast $P^+Q_B^-$ back reaction rate k_b varies between 0.66–0.1 s^{-1} depending on the environment of the RC (see Table 2). Therefore, in this case the apparent equilibrium constant K_2 of the electron transfer $Q_A^-Q_B \leftrightarrow Q_AQ_B^-$ defined as $K_2 = k_b/k_a$ [55], depends essentially on k_b. Table 2 shows the values of K_2, k_b and ΔG, the free energy gap between $Q_A^-Q_B$ and $Q_AQ_B^-$ states of RCs (defined by $K_2 = e^{-\Delta G/kT}$), in different detergent solutions and in membrane fragments, as well. We can see that for RCs in DM, k_b is very slow and thus K_2 and ΔG reach their highest values. When LDAO is added, P^+ relaxation becomes faster, approaching the rate measured in the native state; in the same way, the other parameters depending on k_b decrease (see Table 2).

4. Discussion

In this paper, the isolation and several important functional and structural properties of the *Rc. tenuis* RC are reported. In vivo, this RC is functionally associated with a tetraheme Cyt *c* which is involved in the fast rereduction of the photooxidized Bchl dimer [26]. However the tetraheme Cyt *c* is gradually detached from the RC all along the extraction and purification steps. A slow unbinding has already been observed during the isolation of RCs belonging to other bacterial species like *Rv. gelatinosus* [18], *C. vinosum*, *C. tepidum* and *Cf. aurantiacus* [26]. By contrast, the tetraheme Cyt *c* remains firmly associated in *Rps. viridis* RC in a 1:1 ratio even though high LDAO concentrations is required for the RC purification [56]. Therefore, some structural differences seem to exist between the Cyt *c* binding site of the RCs belonging to the species cited above and that of *Rps. viridis*. Salt bridges observed in the *Rps. viridis* RC structure between residues of the Cyt *c* and those of L and M periplasmic surfaces [57] could be absent in these RCs altogether and/or the hydrophobic contacts could be weaker.

At variance with RC preparations from photosynthetic bacteria belonging to the α-group, such as *Rb. sphaeroides*, *Rb. capsulatus*, *Rsp. rubrum*, those from *Rc. tenuis* and *Rv. gelatinosus* — although not to the same extent — were slowly inactivated when purified in presence of LDAO as seen by their photochemistry and changes in optical spectra. In agreement with previous work [58,59], we have experimental evidence that LDAO dissociates the H subunit from *Rv. gelatinosus* RCs extracted from the wild type as well as from a mutant without the tetraheme Cyt *c* (I. Agalidis and F. Reiss-Husson, unpublished results). This reduced stability and higher sensitivity towards this detergent might reflect differences in the quaternary structure of these RCs. A comparative analysis of the amino acid sequences of the H subunits in these various RCs will be useful in this respect. We also observed that less LDAO and no herbicide was needed to remove UQ from the Q_B site in *Rc. tenuis* as compared to *Rb. sphaeroides*, where a more drastic treatment is needed (i.e., incubation with 1–2% LDAO and 1mM o-phen [60]). The facile liberation of Q_B by LDAO in *Rc. tenuis* is consistent

with the susceptibility of the RC towards this detergent.

4.1. The primary donor of Rc. tenuis

The optical absorption spectra of P and P^+ (Fig. 3) and their corresponding FT Raman spectra (Fig. 5) suggest that, similar to other purple bacterial RCs, the primary donor of *Rc. tenuis* is constituted of two excitonically coupled Bchl *a* molecules, consistent with what is known for other bacterial primary donors. The FT Raman data presented in this work indicate that both Bchl molecules constituting the *Rc. tenuis* primary donor possess one axial ligand each (most likely histidine residues). The determined H-bond pattern for the primary donor is the following: (i) two H-bonded C_2 acetyl carbonyl groups with observed vibrational frequencies at 1618 cm^{-1} and 1635 cm^{-1} and (ii) two C_9 keto carbonyl groups which are free from such protein interactions, vibrating at 1690 cm^{-1} and 1696 cm^{-1} (Fig. 5A).

Sequence alignment of the L subunits of the RCs from several purple bacteria (see Nagashima et al. [61]) shows that the His L168, which forms a H-bond to the P_L C_2 acetyl carbonyl in *Rb. sphaeroides* [62,63] is strongly conserved. The observed vibrational frequency for this acetyl carbonyl of the *Rb. sphaeroides* primary donor is 1620 cm^{-1} [24]; for *Rv. gelatinosus* [32], the corresponding band is 4 cm^{-1} downshifted in frequency as it is for *C. tepidum* [30] indicating a stronger H-bond for these latter species. Thus, a similar H-bond as that found in *Rb. sphaeroides* P is expected on the P_L C_2 acetyl carbonyl group in *Rc. tenuis*, consistent with the observed 1618 cm^{-1} band. Sequence alignment data indicate that His L168 (*Rb. sphaeroides* numbering) is conserved in *Rc. tenuis* (Nagashima, personal communication) and is most likely the H-bond donor to the analogous C_2 acetyl carbonyl of P_L (Table 1) which gives rise to the 1618 cm^{-1} band (Fig. 5A).

On the other hand, the sequence alignment of the M subunits from several purple bacteria [64] shows that *Rb. sphaeroides*, like *Rb. capsulatus*, *Rsp. rubrum*, and *Rv. gelatinosus* possess a Phe at position M197. In the crystal structure of *Rb. sphaeroides* RC [62,63] as well as the FT Raman data on all the above mentioned species [32,65], no H-bond is observed on the P_M C_2 acetyl carbonyl group, vibrating at ca. 1653 cm^{-1}. In contrast, *Rps. viridis*, *Ro. denitrificans*, *Cf. aurantiacus* and *C. tepidum* possess a Tyr residue at position M197 of *Rb. sphaeroides* [30,64]. In the 3-dimensional crystal structure of the *Rps. viridis* RC, this Tyr residue forms a H-bond to the C_2 acetyl carbonyl of P_M [30,57,64,66] The FT Raman spectra of *Cf. aurantiacus* [34] and *C. tepidum* [30] RCs showed that this carbonyl is also H-bonded since the observed vibrational frequency was ca. 1632–1635 cm^{-1}, in agreement with the shifts observed in the FY(M197) RC mutant from *Rb. sphaeroides* [39]. The sequence alignment of the M subunit of *Rc. tenuis* (Nagashima, personal communication) with that of *Rb. sphaeroides* RCs shows that the residue at the equivalent position of Phe(M197) of *Rb. sphaeroides* is indeed a tyrosine. Thus, we propose that this tyrosine residue is the H-bond donor to the P_M C_2 acetyl carbonyl of P in *Rc. tenuis* (Table 1).

It is interesting that some similarities are found between P electronic absorption spectra of *Rc. tenuis* and FY(M197) *Rb. sphaeroides* mutant RCs in vivo: the Q_y band is broad and redshifted at 890 and 880 nm in *Rc. tenuis* and the *Rb. sphaeroides* FY(M197) mutant [39] respectively, when compared to the isolated RCs. As well, the P^+ absorption band is redshifted to 1260 nm in both isolated RCs. These spectral modifications altogether might be the result of the extra H bonding of the dimer to Tyr M197. Nevertheless, the extra H-bonding of P_M C_2 acetyl to TyrM197 does not necessary correlate with a red shift of the near infrared absorption band of P^+. For example, in *C. tepidum* where this extra H bond exists, the P^+ absorption band is blue shifted to 1240 nm [30].

The deduced structure of the microenvironment of the primary donor of *Rc. tenuis* can be correlated with the P/P^+ midpoint redox potential of RCs (Table 1). Specifically, the His-donated H-bond on the acetyl carbonyl of P_L should maintain the redox potential near +500 mV as in the case of *Rb. sphaeroides* RC [29,67]. Moreover, the extra H-bond on the P_M acetyl carbonyl group of *Rc. tenuis* RC, as for *C. tepidum* [30] and for FY(M197) mutant RC from *Rb. sphaeroides* [39], should modestly raise the redox midpoint potential by at least 25 mV. Thus, assuming structural analogy and supposing that the additive effect of H-bonding on the primary donor

redox midpoint potential observed for *Rb. sphaeroides* [36] is also applicable to *Rc. tenuis*, the redox potential of *Rc. tenuis* P should be somewhat higher than that of *Rb. sphaeroides* (see Table 1). This prediction agrees well with our experimental value of 515 ± 20 mV for the membrane fragments. Similar values were determined for the special pair in *C. tepidum* which also has two H-bonded C_2 acetyl carbonyl groups donated by a His and a Tyr residues. The observed redox potential in this case was 526 ± 5 mV for isolated RCs and 502 ± 10 mV for membrane fragments [30].

From the FT Raman results it is also possible to estimate the degree of localization of the resulting positive charge on the primary donor in its cation radical state P^+; in *Rb. sphaeroides* RC, the positive charge distribution was reported to be ca. 80% localized on P_L [24]. Under similar considerations, 69% localization on one Bchl molecule (most probably P_L) of the primary donor of *Rc. tenuis* is estimated which indicates that the + charge is more delocalized over P than it is in *Rb. sphaeroides*. Very similar delocalization was estimated for the primary donor of *C. tepidum* that indeed exhibits a more symmetric protein interaction, i.e., two H-bonded acetyl carbonyl groups [30].

4.2. Quinone acceptor properties

The *Rc. tenuis* RC possesses, like *Rps. viridis* [46], *C. vinosum* [44] and *Rv. gelatinosus* [18] a mixed quinone-acceptor complex with MK as Q_A and UQ as Q_B (Table 1). In a previous report [16] we tried to determine the flash-induced absorption profile of the primary quinone anion in isolated RCs in presence of terbutryn and DAD. However, in these experimental conditions the herbicide was unable to effectively displace Q_B and/or Q_B^- and we obtained an absorption spectrum which was an overlap of both Q_A^- and Q_B^- flash-induced absorption bands (see Fig. 3 in [16]). Therefore in order to avoid the interference of the secondary quinone, we measured the absorption band of Q_A^- in RCs depleted of Q_B. The absorption spectrum obtained now for this bound semimenaquinone 8 species (Fig. 9) is quite similar to those reported for *C. vinosum* [44] and *Cf. aurantiacus* [43]. One may observe that in these three bacterial species the spectra are blue-shifted (thus closer to the in vitro spectrum) as compared to those of *Rps. viridis* [46] and *Rv. gelatinosus* [18] as if, in the latter cases, the electrochromic shifts due to interactions with chlorin pigments were stronger.

We have shown that Q_B activity is strongly dependent on the kind of detergent contained in the RC solution. After purification of the RC in the presence of DM, secondary activity assays in the presence of this surfactant have shown the absence of multiple semiquinone oscillations in intact RCs, as well as the impediment to reconstitute Q_B activity in those devoid of the secondary quinone. These results suggest that the exogeneous Q_6 pool was exclusively partitioned in DM micelles, and UQ_6 molecules could neither move to Q_B site to eventually replace the quinol (QH_2) nor reconstitute Q_B activity in Q_B-less RCs. Nevertheless, LDAO addition allowed the recovery of normal activity at the level of the secondary quinone. The best illustration is the full reconstitution of functional Q_B in RC devoid of secondary activity in presence of a UQ_6 exogeneous pool, demonstrated by the appearance of flash-induced binary oscillations of the semi-ubiquinone (see Fig. 8). In order to understand the different effects of these detergents we should take into account some of their properties, and also what is known about their interactions with photochemical RCs.

Studies of *Rps. viridis* and *Rb. sphaeroides* RCs in crystals [68,69] as well as in micellar solutions of the latter [70] have shown that detergents like LDAO and OG bind essentially to the hydrophobic transmembrane regions of the protein very likely in a monolayer type of arrangement. A similar organization can be expected for DM. LDAO and DM are both nonionic and their alkyl chains are identical. However, the dissacharide head group of DM is bulkier than the amine oxide group of LDAO; accordingly, the DM micelles are non-spherical and bigger ($n = 130$ monomers, $M = 66$ kDa) than those of LDAO ($n = 69$ monomers, $M = 15$ kDa) [71]. The cmc molar values differ also notably [72], being 10 times lower for DM. In solutions containing RCs, UQ_6 molecules should partition between the micelles and the detergent belt of the protein. They might be fully embedded in the DM micelles, but poorly solubilized by the small LDAO ones; in the later case, the remaining UQ pool becomes available to the protein detergent belt, where the regeneration of Q_B could

occur. In a similar fashion LDAO/DM mixed micelles may have a reduced size and a different shape as compared to pure DM, thus being able to share the quinones with the RC.

Another differential effect of the interaction of these detergents with *Rc. tenuis* RC is observed on $P^+Q_B^-$ recombination rate (see Fig. 6). In the presence of DM this light-induced state relaxed very slowly ($k_a = 0.1\ s^{-1}$) (see Table 2), indicating that the electron would take a direct pathway through the protein to return to P^+ [73]. Subsequent addition of LDAO induced the decrease of the P^+ relaxation time to about $0.3\ s^{-1}$, closer to the value determined in the native state (see Table 2). We assume that this change in kinetics reflects a different interaction of DM with the protein, relative to LDAO, which in turn should change the energy level of Q_B/Q_B^-, i.e., the free energy difference ΔG ($P^+Q_A^- - P^+Q_B^-$) (see Table 2). The fact that P^+ rereduction rate could be modulated by the detergents might be an indication of some specific local conformational changes in the microenvironment of pigments induced by the interaction with the bound surfactant molecules.

From the whole kinetic behavior of the secondary acceptor, it turns out that no exchange of UQ or very little occurred at the Q_B site in DM solutions, as if UQ diffusion between DM micelles and RC-detergent complex was almost absent; in contrast, a faster quinone exchange with a weak affinity for Q binding seemed to proceed in presence of LDAO, as in one of the reaction models proposed by Shinkarev and Wraight [74].

In the *Rc. tenuis* RC, as already shown for other bacterial RCs [75], the H^+ concentration is capable of modifying P^+ rereduction rate after a flash. Preliminary $P^+Q_AQ_B^-$ recombination reaction rate measurements in DM solution, at several pH values between 6 and 9.5, have shown an increase in rate from 0.043 to $0.27\ s^{-1}$ (I. Agalidis, unpublished results). From these rate constants, it turns out that the free energy gap between $P^+Q_A^-$ and $P^+Q_B^-$ states below pH 8 is larger than 100 mV. Then it is reasonable to assume that the pathway of $P^+Q_B^-$ recombination essentially occurs by a tunnelling mechanism to the ground state [73]; conversely, at pH values higher than 8 the indirect pathway through the higher lying $P^+Q_A^-$ state seems to dominate.

In the *Rc. tenuis* RC the Q_A^- to Q_B electron transfer was inhibited at a very low concentration of o-phen with $I_{50} = 10\ \mu M$. Similar values were determined for *Rps. viridis* [49,50] and *Rv. gelatinosus* [51] RCs. This sensitivity distinguishes these species altogether with respect to *Rb. sphaeroides* and *Rb. capsulatus* which have I_{50} values in the range 100–200 μM [52–54]. The degree of inhibition by o-phen was correlated with the residue present in the position L226 [54]; bacteria which have a Thr residue in the position L226 are weakly inhibited, whereas those which have an Ala residue at this position such as *Rps. viridis* [50] and the ThrL226 → Ala *Rb. capsulatus* mutant [54], or even a Ser residue, like in *Rv. gelatinosus* [51], were shown to be highly sensitive. It was supposed that a smaller residue in position L226 may allow an easier diffusion of o-phen to its binding site [54]. These results are now extended to *Rc. tenuis*, where L226 is also an Ala residue (Nagashima, personal comunication) and which at the same time is strongly inhibited by o-phen (Table 1). Structural similarities of the Q_B site between *Rc. tenuis* and *Rps. viridis* are reinforced by these observations.

Acknowledgements

We are grateful to Dr. K. Nagashima who kindly provided us with the unpublished primary sequences of the L and M subunits of *Rc. tenuis* reaction center. We thank Dr. P. Sebban and Dr. C. Vernotte for their useful discussion and the critical reading of the manuscript. We are indebted to Mrs. M.C. Gonet for her assistance in growing *Rc. tenuis* cells and preparing the membranes.

References

[1] C.R. Woese, Microbiol. Rev. 51 (1987) 221–271.
[2] A. Willems, M. Gillis, J. De Ley, Intern. J. Syst. Bacteriol. 41 (1991) 65–73.
[3] B. Wakim, J.R. Golecki, J. Oelze, FEMS Microbiol. Lett. 4 (1978) 199–201.
[4] Q.H. Hu, R.A. Brunisholz, G. Frank, H. Zuber, Eur. J. Biochem. 238 (1996) 381–390.
[5] L. Menin, P. Parot, B. Scoepp, P. Richaud, A. Verméglio, in: P.E. Mathis (Ed.), Photosynthesis: from Light to Biosphere, vol. II, Kluwer Academic Publishers, Dordrecht, The Netherlands, 1995.
[6] R.G. Bartsch, Biochim. Biophys. Acta 1058 (1991) 28–30.

[7] I. Rayment, G. Wesenberg, T.E. Meyer, M.A. Cusanovich, H.M. Holden, J. Mol. Biol. 228 (1992) 672–686.
[8] B. Schoepp, P. Parot, L. Menin, J. Gaillard, P. Richaud, A. Verméglio, Biochemistry 34 (1995) 11736–11742.
[9] T.E. Meyer, T.J. Donohue, in: R.E. Blankenship, M.T. Madigan, C.E. Bauer (Eds.), Anoxygenic Photosynthetic Bacteria Kluwer Academic Publishers, The Netherlands, 1995.
[10] A. Hochkoeppler, S. Ciurli, G. Venturoli, D. Zannoni, FEBS Lett. 357 (1995) 70–74.
[11] S.J. Kennel, R.G. Bartsch, M.D. Kamen, Biophys. J. 12 (1972) 882–896.
[12] T.E. Meyer, J.J. van Beeumen, R.P. Ambler, M.A. Cusanovich, in: Baltcheffski (Ed.), Origin and Evolution of Biological Energy Conversion, VCH Publishers, New York, 1996.
[13] K.V.P. Nagashima, K. Shimada, K. Matsuura, in: P. Mathis (Ed.), Photosynthesis: from Light to Biosphere, vol. II, Kluwer Academic Publishers, Dordrecht, 1995, pp. 599-602.
[14] V.P. Kenji, K. Nagashima, K. Matsuura, Photosynth. Res. 36 (1993) 185–191.
[15] I. Agalidis, P. Sebban, Biochim. Biophys. Acta 1232 (1995) 180–186.
[16] I. Agalidis, F. Reiss-Husson, in: P. Mathis (Ed.), Photosynthesis: From Light to Biosphere, vol. I, Kluwer Academic Publishers, Dordrecht, 1995.
[17] I. Agalidis, E. Rivas, F. Reiss-Husson, Photosynth. Res. 23 (1990) 249–255.
[18] I. Agalidis, F. Reiss-Husson, Biochim. Biophys. Acta 1098 (1992) 201–208.
[19] P.E. Thomas, D. Ryan, W. Levin, Anal. Biochem. 76 (1976) 168–176.
[20] S.C. Straley, W.W. Parson, D.C. Mauzerall, R.K. Clayton, Biochim. Biophys. Acta 305 (1973) 597–609.
[21] E.A. Berry, B.L. Trumpower, Anal. Biochem. 161 (1987) 1–15.
[22] W.M. Clark, in: W.M. Clark (Ed.), Oxidation-Reduction Potentials of Organic Systems, The Williams and Wilkins Company, Baltimore, 1960.
[23] P. Maroti, D.K. Hanson, L. Baciou, M. Schiffer, P. Sebban, Proc. Natl. Acad. Sci. U.S.A. 91 (1994) 5617–5621.
[24] T.A. Mattioli, A. Hoffmann, B. Robert, M. Lutz, Biochemistry 30 (1991) 4648–4654.
[25] M.Y. Okamura, G. Feher, G.N. Nelson, in: Govindjee (Ed.), Photosynthesis: Energy Conservation by Plants and Bacteria, Academic Press, New York, 1982.
[26] W. Nitschke, S.M. Dracheva, in: R.E. Blankenship, M.T. Madigan, C.E. Bauer (Eds.), Anoxygenic Photosynthetic Bacteria Kluwer Academic Publishers, Dordrecht, 1995.
[27] W.W. Parson, R.J. Cogdell, Biochim. Biophys. Acta 416 (1975) 105–149.
[28] S. Wang, S. Lin, X. Lin, N.W. Woodbury, J.P. Allen, Photosynth. Res. 42 (1994) 203–215.
[29] L.M.P. Beekman, R.W. Visschers, R. Monshouwer, M. Heerdawson, T.A. Mattioli, P. Mcglynn, C.N. Hunter, B. Robert, I.H.M. Vanstokkum, R. van Grondelle, M.R. Jones, Biochemistry 34 (1995) 14712–14721.
[30] A. Ivancich, M. Kobayashi, F. Drepper, I. Fathir, T. Saito, T. Nozawa, T.A. Mattioli, Biochemistry 35 (1996) 10529–10538.
[31] P.L. Dutton, J.B. Jackson, Eur. J. Biochem. 30 (1972) 495–510.
[32] I. Agalidis, B. Robert, T. Mattioli, F. Reiss-Husson, in: J. Breton, A. Verméglio (Eds.), The Photosynthetic Bacterial Reaction Center: Structure, Spectroscopy and Dynamics, Plenum Press, New York, 1992.
[33] U. Feiler, D. Albouy, B. Robert, T.A. Mattioli, Biochemistry 34 (1995) 11099–11105.
[34] A. Ivancich, R. Feick, A. Ertlmaier, T.A. Mattioli, Biochemistry 35 (1996) 6126–6135.
[35] T.A. Mattioli, J.C. Williams, J.P. Allen, B. Robert, Biochemistry 33 (1994) 1636–1643.
[36] T.A. Mattioli, X. Lin, J.P. Allen, J.C. Williams, Biochemistry 34 (1995) 6142–6152.
[37] T.M. Cotton, R.P. Van Duyne, J. Am. Chem. Soc. 103 (1981) 6020–6026.
[38] M. Lutz, R.J.H. Clark, R.E. Hester (Eds.), Advances in Infrared and Raman Spectroscopy, vol. 11, Wiley, New York, 1984.
[39] J. Wachtveitl, J.W. Farchaus, R. Das, M. Lutz, B. Robert, T.A. Mattioli, Biochemistry 32 (1993) 12875–12886.
[40] J.F. Imhoff, FEMS Microbiol. Lett. 25 (1984) 85–89.
[41] A. Verméglio, Biochim. Biophys. Acta 459 (1977) 516–524.
[42] C.A. Wraight, Biochim. Biophys. Acta 459 (1977) 525–531.
[43] H. Vasmel, J. Amesz, Biochim. Biophys. Acta 724 (1983) 118–122.
[44] J. Romijn, J. Amesz, Biochim. Biophys. Acta 461 (1977) 327–338.
[45] P.S. Rao, E. Hayon, Biochim. Biophys. Acta 724 (1983) 118–122.
[46] R.J. Shopes, C.A. Wraight, Biochim. Biophys. Acta 806 (1985) 348–356.
[47] T. Nozawa, J.T. Trost, T. Fukada, M. Hatano, J.D. McManus, R.E. Blankenship, Biochim. Biophys. Acta 894 (1987) 468–476.
[48] T. Leguijt, P. Parot, A. Verméglio, W. Crielaard, K.J. Hellingwerf, Biochim. Biophys. Acta 1183 (1993) 292–300.
[49] R.J. Shopes, C.A. Wraight, in: J. Biggins (Ed.), Proceedings of VIIth International Congress on Photosynthesis Martinus Nijhoff, The Hague, 1987.
[50] I. Sinning, H. Michel, P. Mathis, A.W. Rutherford, Biochemistry 28 (1989) 5544–5553.
[51] S. Ouchane, M. Picaud, C. Astier, FEBS Lett. 374 (1995) 130–134.
[52] R.R. Stein, A.I. Catellvi, J.P. Bogacz, C.A. Wraight, J. Cell. Biochem. 24 (1984) 243–259.
[53] R.J. Debus, G. Feher, M.Y. Okamura, Biochemistry 24 (1985) 2488–2500.
[54] L. Baciou, E.J. Bylina, P. Sebban, Biophys. J. 65 (1993) 652–660.

[55] L.J. Mancino, D.P. Dean, R.E. Blankenship, Biochim. Biophys. Acta 764 (1984) 46–54.
[56] H. Michel, J. Mol. Biol. 158 (1982) 567–572.
[57] J. Deisenhofer, O. Epp, I. Sinning, H. Michel, J. Mol. Biol. 246 (1995) 429–457.
[58] B.J. Clayton, R.K. Clayton, Biochim. Biophys. Acta 50 (1978) 470–477.
[59] A. Fukushima, K. Matsuura, K. Shimada, T. Satoh, Biochim. Biophys. Acta 993 (1988) 399–405.
[60] M.Y. Okamura, R.A. Isaacson, G. Feher, Proc. Natl. Acad. Sci. USA 72 (1975) 3491–3495.
[61] K.V.P. Nagashima, K. Matsuura, S. Ohyama, K. Shimada, J. Biol. Chem. 269 (1994) 1–8.
[62] U. Ermler, G. Fritzsch, S.K. Buchanan, H. Michel, Structure 2 (1994) 925–936.
[63] B. Arnoux, F. Reiss-Husson, Eur. Biophys. J. 24 (1996) 233–242.
[64] K.V.P. Nagashima, K. Shimada, K. Matsuura, Photosynth. Res. 36 (1993) 185–191.
[65] T.A. Mattioli, B. Robert, M. Lutz, in: J. Breton, A. Verméglio (Eds.), The Photosynthetic Bacterial Reaction Center, vol. I, Plenum Press, New York, 1992.
[66] J. Deisenhofer, H. Michel, EMBO J. 8 (1989) 47–54.
[67] J.C. Williams, R.G. Alden, H.A. Murchinson, J.M. Peloquin, N.W. Woodbury, J.P. Allen, Biochemistry 31 (1992) 11029–11037.
[68] M. Roth, A. Lewit-Bentley, M. Michel, J. Deisenhofer, R. Huber, D. Oesterhelt, Nature 340 (1989) 659–661.
[69] M. Roth, B. Arnoux, A. Ducruix, F. Reiss-Husson, Biochemistry 30 (1991) 9403–9413.
[70] J.U. Moller, M. Le Maire, J. Biol. Chem. 268 (1993) 18659–18672.
[71] P.A. Timmins, M. Leonhard, H.U. Weltzien, T. Wacker, W. Welte, FEBS Lett. 238 (1988) 361–368.
[72] J.M. Neugebauer, Meth. Enzymol. 182 (1990) 239–253.
[73] A. Labhan, M.L. Paddock, P.H. McPherson, M.Y. Okamura, G. Feher, J. Phys. Chem. 98 (1994) 3417–3423.
[74] V.P. Shinkarev, C.A. Wraight, in: J. Deisenhofer, J.R. Norris (Eds.), The Photosynthetic Reaction Center, vol. I, Academic Press, New York, 1993.
[75] P. Sebban, P. Maroti, D.K. Hanson, Biochimie 77 (1995) 677–684.
[76] P.L. Dutton, Biochim. Biophys. Acta 226 (1971) 63–80.
[77] R.C. Prince, J.S. Leigh, P.C. Dutton, Biochim. Biophys. Acta 440 (1976) 622–636.
[78] B. Dohse, P. Mathis, J. Wachtveitl, E. Laussermair, S. Iwata, H. Michel, D. Oesterhelt, Biochemistry 34 (1995) 11335–11343.
[79] G. Venturoli, D. Zannoni, Eur. J. Biochem. 178 (1988) 503–50980.
[80] V.A. Shuvalov, A.Ya. Shkuropatov, S.M. Kulakova, M.A. Ismailov, U.A. Shkuropatova, Biochim. Biophys. acta 849 (1986) 337–346.
[81] S. Ouchane, M. Picaud, F. Reiss, C. Vernotte, C. Astier, Mol. Gen. Genet. 252 (1996) 379–385.
[82] J.A. Shiozawa, F. Lottspeich, R. Feick, Eur. J. Biochem. 167 (1987) 595–600.
[83] M.B. Hale, R.E. Blankenship, R.C. Fuller, Biochim. Biophys. Acta 723 (1983) 376–382.